

E7-2001-37

J.Staňo, V.A.Skuratov, M.Žiška\*

CHARGE DEEP LEVEL TRANSIENT  
SPECTROSCOPY STUDY OF 3 ÷ 7 MEV/AMU ION  
AND FAST NEUTRON IRRADIATION-INDUCED  
CHANGES IN MOS STRUCTURES

---

\*Department of Microelectronics, Faculty of Electrical Engineering  
and Information Technology, Bratislava, Slovak Republic



## Introduction

Radiation damage-induced changes in the electrical properties of MOS circuits are determined by a combined structural response of the oxide and semiconductor layers and of the interface region. The main materials forming MOS structures – silicon and silicon oxide – are known to have different sensitivity to ionizing radiation, especially at high electronic stopping powers. As known, starting from a certain threshold value, the ionizing energy loss begins to play a dominant role in damage formation in both amorphous and crystalline SiO<sub>2</sub> in comparison with elastic collisions [1, 2]. In particular, continuous radiation defects, associated with inelastic energy loss, latent tracks, have been observed in quartz at  $(dE/dx)_{ion} > 1.6$  keV/nm. [3] At the same time the electronic energy deposition is inefficient for direct defect creation in silicon even at very high ionizing densities,  $(dE/dx)_{ion} = 28$  keV/nm. [4]. A specific effect due to the high electronic excitation, latent track formation, was observed only after irradiation of silicon with tens MeV fullerenes, when the electronic stopping power reaches extremely high values, about 50 keV/nm [5, 6]. This fact does not exclude that dense ionization together with atomic displacements can affect evolution of defects in irradiated silicon and the final electrical properties of MOS circuits. Despite the obvious interest, first of all for space electronics, radiation-induced degradation processes of MOS circuits exposed under such conditions, i.e. with high energy heavy ions, are practically unstudied. The first preliminary data about radiation defects in MOS structures irradiated with Bismuth and Krypton swift ions were reported in [7]. In the present work, the Charge Deep Level Transient Spectroscopy (Q-DLTS) [8] and Feedback Charge Capacitance –Voltage (C-V) [9] techniques were used to characterize radiation defects in MOS structures irradiated by hundred MeV heavy ions in a wide range of electronic and nuclear energy losses, and by fast neutrons.

## Experimental

N-type antimony doped (100) oriented silicon wafer with a resistivity of 0.009 - 0.02 Ωcm and thickness of 300 μm was used as a substrate of the MOS structure. An epitaxial layer with resistivity 3 Ωcm (doping concentration  $1.66 \times 10^{15}$  cm<sup>-3</sup>) and thickness of 5÷8 μm was grown on the substrate wafer. In all samples, the gate layers were grown by thermal oxidation in an atmosphere of dry oxygen at 1050°C for 90 minutes. The thickness of the layer was about 100 nm. Aluminium square contacts with sizes from 0.5 to 0.9 mm were vapour deposited and patterned photolithographically. The ohmic contact from the backside of the wafer has been

prepared by vapour deposition of Al. After manufacturing the MOS structure, the samples were annealed in  $N_2+H_2$  at 460°C for 20 minutes. The samples were irradiated with 710 MeV Bi, 245 MeV Kr, 280 MeV and 155 MeV Ar ions and with fast ( $E_n > 0.1$  MeV) neutrons. Heavy ion irradiations were carried out at room (RT) and liquid nitrogen (NT) temperatures on the ion beam transport line for applied research of the U-400 cyclotron at FLNR JINR, Dubna [10]. In the case of experiments with 710 MeV Bi and 155 MeV Ar ions, some samples were covered by aluminium foils with thicknesses 9.5 and 18  $\mu m$  in order to modify the ion energy. Under exposure, the ion beam flux was limited to  $2 \times 10^8 \text{ cm}^{-2} \text{ s}^{-1}$  to avoid possible overheating of the targets. The ion beam homogeneity not worse than 5% on the irradiated surface was reached using low-frequency ( $\approx 100$  Hz) beam scanning in horizontal and vertical directions. The main characteristics of irradiation, such as particle type and incident energy, absorber thickness, ion projected range, fluence range and irradiation temperature, are given in table 1. The projected range values show that the ions were stopped in the silicon substrate.

| Ion type | Energy, MeV | Al absorber thickness, $\mu m$ | Ion projected range, $\mu m$ | Fluence, $cm^{-2}$                                     | Irradiation temperature |
|----------|-------------|--------------------------------|------------------------------|--|-------------------------|
| Ar       | 280         | 0                              | 80.89                        | $10^9$   | RT, NT                  |
|          |             |                                |                              | $10^{10}, 10^{11}$                                     | RT                      |
|          | 155         | 0                              | 39.98                        | $10^{10}$  | RT, NT                  |
|          | 115         | 9.5                            | 28.97                        | $10^{10}$  | RT                      |
| Kr       | 77          | 18                             | 19.48                        | $10^{10}$  | RT                      |
|          | 245         | 0                              | 31.23                        | $10^9, 10^{10}, 10^{11}$                               | RT                      |
| Bi       | 710         | 0                              | 43.33                        | $2.4 \times 10^8$                                      | NT                      |
|          |             |                                |                              | $1.2 \times 10^9, 1.2 \times 10^{10}$                  | RT, NT                  |
|          | 469         | 9.5                            | 32.48                        | $10^9$   | RT                      |
| Neutrons | 269         | 18                             | 22.85                        | $10^9$   | RT                      |
|          | >0.1 MeV    | -                              | -                            | $7 \times 10^{12}, 10^{13}, 5 \times 10^{13}, 10^{14}$ | RT                      |

Table 1. Main parameters of the ion and neutron irradiation

To irradiate and test the targets at low temperatures, we used a cryostat system operating at 77-400 K. Initially, MOS structures were placed in the cryostat at an angle of 45 degrees with respect to the beam direction and connected with measurement pins. Then the cryostat was mounted into the irradiation chamber of the accelerator and evacuated. After cooling to 77 K and irradiation, the vacuum volumes of the ion beam line and cryostat system were separated without vacuum loss in the cryostat and the latter was connected to the Q-DLTS spectrometer for measurements.

Neutron irradiation was performed at room temperature using the large-scale samples irradiation facility at the IBR-2 reactor in the Laboratory of Neutron Physics, JINR, Dubna, and described elsewhere [11]. The fluence of fast ( $E > 0.1$  MeV) neutrons and  $\gamma$ -irradiation dose were monitored with accuracy not worse than 30%. The range of neutron fluences is also given in table 1. To prevent irradiation with thermal neutrons and avoid undesirable additional activation the samples were protected with boron carbide ( $B_4C$ ) layer.

Charge DLTS and C-V measurements were carried out with the time-domain spectrometer SP-DLS-02 working in two regimes: charge deep level transient spectrometer and complementary feedback-charge capacitance-voltage meter.

## Results and discussion

### I. C-V characterisation of MOS structures

In the second mode of the time-domain spectrometer, characteristic C-V curves of samples irradiated with high energy ions and neutrons were obtained. The radiation-induced changes of the C-V plot against the virgin (non-irradiated) curve are shown in figure 1. As it was

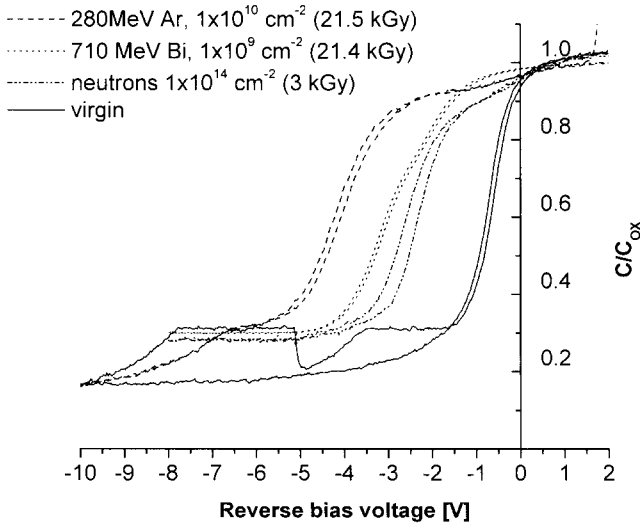


Fig. 1. C-V curves at RT of the samples irradiated with 280 MeV Ar and 710 MeV Bi ions with fluences  $1 \times 10^{10}$  and  $1 \times 10^9 \text{ cm}^{-2}$ , respectively, which corresponds to absorbed dose in  $SiO_2$  of about 21 kGy.

found, swift heavy ion bombardment at room temperature in all cases results in the shift of the curve toward the negative voltage, showing the presence of a positive effective charge density in SiO<sub>2</sub> layer. A strong temperature dependence of the shape of the C-V was registered too. The flat-band voltage level shift of the C-V curves at NT is smaller as that as at RT. The change of the flat-band voltage  $U_{FB}$  of the MOS structure is characterized by accumulation of the fixed charge due to irradiation-induced ionized traps in the oxide layer. The total effective defect charge density can be calculated from the following equation:

$$N_{ox} = \frac{U_{FB} C_{OX}}{q} = \frac{\epsilon_0 \epsilon U_{FB}}{h_{ox} q},$$

where  $U_{FB}$ ,  $C_{ox}$  are the flat-band voltage and capacitance of the oxide,  $h_{ox}$  is the thickness of the oxide,  $\epsilon_0$ ,  $\epsilon$  are the permittivities of vacuum and of the oxide layer, and  $q$  is the electron charge.

The  $N_{ox}$  values determined for Ar, Kr and Bi ions and neutrons at different irradiation temperatures,  $T_{irr}$ , are summarized in table 2. Specific electronic ( $S_e$ ) and nuclear energy

| Ions | Energy, MeV         | Fluence, cm <sup>-2</sup> | $T_{irr}$            | $S_e$ keV/nm | $S_n$ keV/nm          | $D$ , Gy/ion          | $D$ , Gy             | $U_{FB}$ , V         | $N_{ox}$ , cm <sup>-2</sup> |
|------|---------------------|---------------------------|----------------------|--------------|-----------------------|-----------------------|----------------------|----------------------|-----------------------------|
| Ar   | 280                 | 10 <sup>9</sup>           | RT                   | 3.0          | 0.0011                | 2.15x10 <sup>-6</sup> | 2.15x10 <sup>3</sup> | -1.1                 | 2.5x10 <sup>11</sup>        |
|      |                     |                           | NT                   |              |                       |                       | -                    | -1.1                 | 2.5x10 <sup>11</sup>        |
|      | 155                 | 10 <sup>10</sup>          | RT                   | 3.9          | 0.003                 | 2.67x10 <sup>-6</sup> | 2.15x10 <sup>4</sup> | -4.3                 | 8.4x10 <sup>11</sup>        |
|      |                     |                           | RT                   |              |                       |                       | 2.15x10 <sup>5</sup> | -8.7                 | 1.7x10 <sup>12</sup>        |
|      |                     | NT                        | 2.67x10 <sup>4</sup> |              |                       |                       | -4.2                 | 8.2x10 <sup>11</sup> |                             |
|      |                     | NT                        | -                    |              |                       |                       | -4.5                 | 8.9x10 <sup>11</sup> |                             |
| 115  | 10 <sup>10</sup>    | RT                        | 4.2                  | 0.0039       | 2.87x10 <sup>-6</sup> | 2.87x10 <sup>4</sup>  | -3.6                 | 7.2x10 <sup>11</sup> |                             |
|      | 77                  | 10 <sup>10</sup>          | RT                   | 4.5          | 0.0055                | 3.14x10 <sup>-6</sup> | 3.14x10 <sup>4</sup> | -3.9                 | 7.9x10 <sup>11</sup>        |
| Kr   | 245                 | 10 <sup>9</sup>           | RT                   | 10.5         | 0.0142                | 6.77x10 <sup>-6</sup> | 6.77x10 <sup>3</sup> | -2.0                 | 4.0x10 <sup>11</sup>        |
|      |                     | 10 <sup>10</sup>          | RT                   |              |                       |                       | 6.77x10 <sup>4</sup> | -5.7                 | 1.1x10 <sup>12</sup>        |
|      |                     | 10 <sup>11</sup>          | RT                   |              |                       |                       | 6.77x10 <sup>5</sup> | -10.2                | 2.0x10 <sup>12</sup>        |
| Bi   | 710                 | 2.4x10 <sup>8</sup>       | NT                   | 25.2         | 0.05                  | 1.79x10 <sup>-5</sup> | 4.2x10 <sup>3</sup>  | -1.5                 | 3.2x10 <sup>11</sup>        |
|      |                     |                           | RT                   |              |                       |                       | 2.14x10 <sup>4</sup> | -2.9                 | 5.7x10 <sup>11</sup>        |
|      |                     | 1.2x10 <sup>9</sup>       | NT                   |              |                       |                       | -                    | -3.5                 | 7.0x10 <sup>11</sup>        |
|      |                     |                           | RT                   |              |                       |                       | 2.14x10 <sup>5</sup> | -5.5                 | 1.1x10 <sup>12</sup>        |
|      |                     |                           | NT                   |              |                       |                       | -                    | -6.8                 | 1.3x10 <sup>12</sup>        |
|      |                     |                           | RT                   |              |                       |                       | 2.04x10 <sup>4</sup> | -1.8                 | 3.6x10 <sup>11</sup>        |
| 469  | 1.2x10 <sup>9</sup> | RT                        | 24                   | 0.0705       | 1.7x10 <sup>-5</sup>  | 1.80x10 <sup>4</sup>  | -1.9                 | 3.8x10 <sup>11</sup> |                             |
|      | 269                 | 1.2x10 <sup>9</sup>       | RT                   | 21           | 0.0106                | 1.50x10 <sup>-5</sup> | 1.80x10 <sup>4</sup> | -1.9                 | 3.8x10 <sup>11</sup>        |
| n    | > 0.1MeV            | 7x10 <sup>12</sup>        | RT                   | -            | -                     | 3x10 <sup>-11</sup>   | 2.1x10 <sup>2</sup>  | -0.8                 | 1.6x10 <sup>11</sup>        |
|      |                     | 10 <sup>13</sup>          | RT                   | -            | -                     | -                     | 3x10 <sup>2</sup>    | -1.0                 | 2.0x10 <sup>11</sup>        |
|      |                     | 5x10 <sup>13</sup>        | RT                   | -            | -                     | -                     | 1.65x10 <sup>3</sup> | -2.0                 | 3.9x10 <sup>11</sup>        |
|      |                     | 10 <sup>14</sup>          | RT                   | -            | -                     | -                     | 3.0x10 <sup>3</sup>  | -2.0                 | 3.9x10 <sup>11</sup>        |
|      |                     | 10 <sup>14</sup>          | RT                   | -            | -                     | -                     | 3.0x10 <sup>3</sup>  | -2.0                 | 3.9x10 <sup>11</sup>        |

Table 2. The flat-band voltage shift and corresponding total effective charge density in SiO<sub>2</sub> layer.

depositions ( $S_n$ ) and the absorbed dose in  $\text{SiO}_2$  are given in this table 2, too. For more evidence, figure 2 presents the effective charge density in the oxide layer as a function of the absorbed dose for samples irradiated at room temperature. As one can see from table 2 and figure 2, the main peculiarity in the experimental data is a relatively low value of  $N_{\text{ox}}$  for bismuth in comparison with other ions. Evidently, defects acting as traps for charge carriers are created in  $\text{SiO}_2$  with a

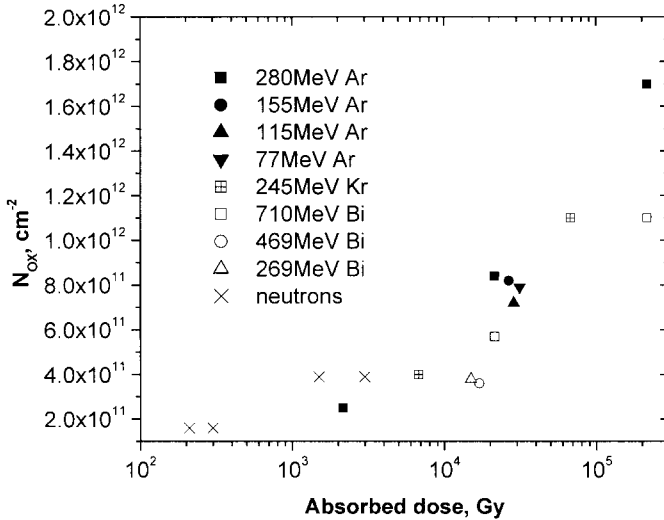


Fig. 2. Effective charge density in the  $\text{SiO}_2$  layer versus absorbed dose after irradiation with high energy heavy ions and neutrons at 300 K.

lower efficiency under dense electronic excitations. One should note that the nuclear stopping power defining the amount of defects created in elastic collisions is about 5 times higher for 710 MeV Bi than, in particular, for 280 MeV Ar ions at the same absorbed dose.

Taking into account the ion fluences used in our study,  $\leq 10^{11} \text{ cm}^{-2}$ , one can state that structural defects in  $\text{SiO}_2$  layer are concentrated predominantly in single, separate track regions. The estimations of the fluence value,  $F_{I_{\text{over}}}$ , corresponding to tracks overlapping, were based on the track size and damage cross-section values determined in [4] over a broad range of electronic stopping powers ( $1.6 \text{ keV/nm} < S_e < 27.8 \text{ keV/nm}$ ). For example,  $F_{I_{\text{over}}}$  is close to  $5 \times 10^{11} \text{ cm}^{-2}$  in the case of 5.0 MeV/amu lead ions. Our experimental data demonstrate that the high level of

ionizing density strongly affected the amount of electrically active defects in the damaged zones surrounding the ion trajectory. Probably, this effect has a threshold character, which requires more detailed studies of the  $N_{ox}(D)$  dependence.

The changes in C-V plots measured on neutron irradiated structures are due to accumulation of point defects created in elastic collisions, which is typical for fluences up to  $10^{18}$   $\text{cm}^{-2}$  [3]. This is why they could not be compared directly with data obtained with swift heavy ions.

## 2. Charge DLTS spectra study of irradiated MOS capacitors

No deep levels were observed in virgin samples (before irradiation) in a wide range of reverse bias voltages and filling pulses. Figure 3 shows Q-DLTS spectra from the silicon substrate of MOS structures irradiated by 710 MeV Bi ions; the spectra are typical for all

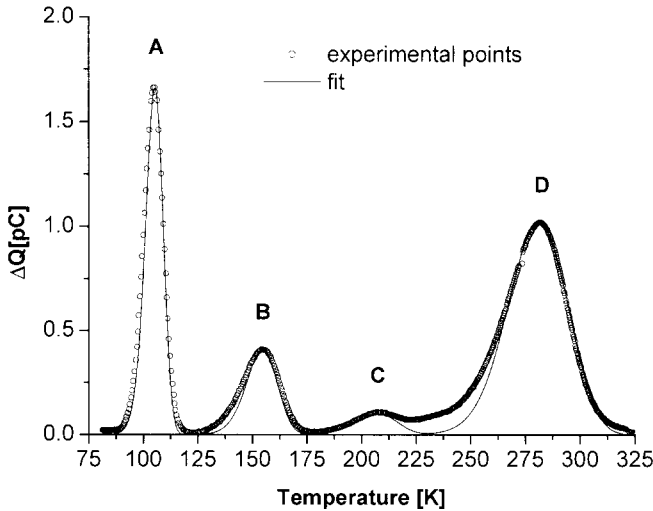


Fig. 3. Q-DLTS spectrum of the sample irradiated by 710 MeV Bi ions at the dose  $1 \times 10^9$  ions/ $\text{cm}^2$  and corresponding theoretical fit with parameters for peak A:  $E_c - E = 0.164$  eV,  $\sigma = 1.8 \times 10^{-14}$   $\text{cm}^2$ ; peak B:  $E_c - E = 0.20$  eV,  $\sigma = 3.88 \times 10^{-16}$   $\text{cm}^2$ ; peak C:  $E_c - E = 0.274$  eV,  $\sigma = 2.96 \times 10^{-16}$   $\text{cm}^2$ ; peak D:  $E_c - E = 0.397$  eV,  $\sigma = 4.54 \times 10^{-16}$   $\text{cm}^2$ . Measurement parameters were set to period = 1 ms, filling pulse = 0.1 ms and  $\tau = 0.1$  ms.



projectiles. The spectra are composed of peaks attributed to the well-known radiation defects such as vacancy-oxygen complex (VO or A-center) (peak “A”), double negative charged divacancy ( $W^-$ ) (peak “B”), negative charged divacancy ( $W^-$ ) and probably donor related center (VD) (peak “D”), see for example in [12]. Peak “C” occurring at 0.274 eV below the conduction band is due to an impurity-related center, possibly containing carbon and/or copper [12]. For estimation of the energy level  $\Delta E$  and the emission cross-section  $\sigma$  of each peak we used the Arrhenius plot approximation of the  $\ln(T_m^2 \tau_m)$  versus  $1000/T_m$  dependence, where  $1/\tau_m = v_i N_c \sigma \exp(-\Delta E/kT_m)$ . Accordingly, we made three temperature scans with various time windows corresponding to  $\tau = 0.05, 0.1$  and  $1$  ms. We detected clear spectra of discrete levels only in the case when the sample was reverse biased at a voltage level corresponded to the inversion mode of the MOS structure at room temperature. If the sample was cooled no inversion was occurred and structures were in deep depletion. Otherwise, the spectra were perturbed by a continuous compound signal from  $SiO_2$  and  $Si/SiO_2$  interface states (their study was not the aim of this work). The requirement to make the measurements in this reverse voltage range disabled us from finding the  $W^-$  and  $W^-$  level concentrations with good accuracy because in the temperature range above 250 K, where the signal from  $W^-$  was detected, there were no significant capacitance changes. To perform a correct calculation of the concentration it is necessary to know C-V characteristic at the temperature peak maximum of individual levels. Therefore, we only determined the concentrations of A-centers in the Si epitaxial layer. The algorithm used for the evaluation of deep level concentration is described elsewhere [13]. Figure 4 shows the concentration of A-centers,  $n_{VO}$ , in Ar (280 MeV), Bi (710, 469, 269 MeV) and neutron irradiated MOS structures via total amount of vacancies predicted by the SRIM code for heavy ions and damage cross-section data for a composed neutron spectrum of different neutron energy groups [14]. The total neutron damage cross-section in our case (beam N 3 of IBR-2 reactor) was equal to  $2.28 \times 10^{-21} \text{ cm}^{-2}$ . For comparison, this value for  $^{235}\text{U}$  fission spectrum reported by Greenwood [15] is  $2.96 \times 10^{-21} \text{ cm}^{-2}$ . In all calculations a displacement energy threshold of 13 eV was used. The data presented in this figure demonstrate no dependence of VO defects number on the inelastic energy loss of heavy ions in silicon, which is consistent with previous studies in [4]. Within the range of electronic stopping powers,  $S_e = 2.7 \div 22.3 \text{ keV/nm}$ , the experimentally determined values of  $n_{VO}$  are about one percent of the total number of vacancies for all heavy ions. We can not ascribe the observed difference in the data taken at the same damage level to the  $S_e$  effect due to an irregular nature of the  $n_{VO}(S_e)$  dependence. One should note also that A-center

concentration in neutron irradiated MOS is lower but rather close to that measured for heavy ions. The Q-DLTS spectra measured in samples exposed at 80 and 300 K show an increase in VO concentration in a practically identical ratio for both bismuth and argon ions (see Fig. 4).

Similar amounts of VO defects created by Ar, Bi ions and neutrons per particle-induced vacancy is a rather unexpected result, taking into account the difference in recoil spectra generated by these projectiles. This can be seen from table 3, where the parameter characterizing

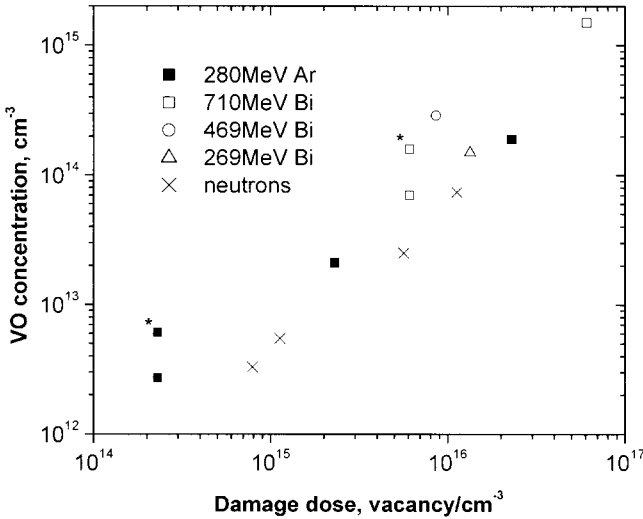


Fig. 4. A-center concentration as a function of the damage dose (data points marked with \* correspond to irradiation at NT).

the PKA (primary knock-on atom) spectra, mean number of knock-on atoms per unit length are listed. The total number of vacancies obtained using this method in comparison with SRIM code prediction is given in table 3, too. By the estimates, the overwhelming majority of radiation defects are created in atomic collision cascades in the case of Bi ion bombardment. Assuming that recombination phenomena affect the number of point defects in the collision cascade region, we could expect a distinct difference in A-center density for Ar and Bi ions, as well as for neutrons, like it was observed for silicon irradiated with 0.4÷8.0 MeV ions [12]. A systematic DLTS study undertaken there revealed that for a given density of energy deposited in elastic

collisions, heavy ions produced less vacancies free to migrate, and fewer VO centers were formed than for light ions. It is suggested that point defect annihilation due to fast diffusing

| Ions | Energy, MeV | Number of vacancies, vac./ion/cm <sup>3</sup> | $N_{pka}$ , ion <sup>-1</sup> Å <sup>-1</sup> |
|------|-------------|---|---|
| Ar   | 280         | $2.3 \times 10^5$                             | $5.2 \times 10^{-4}$                          |
| Bi   | 710         | $6.1 \times 10^6$                             | $6.1 \times 10^{-3}$                          |
| n    | >0.1MeV     | $1.13 \times 10^2$                            |   |

*Table 3. Vacancy production and the mean number of PKA atoms,  $N_{pka}$  in Si target, predicted by SRIM 2000 code.*

interstitials, is enhanced when the collision cascades are generated sufficiently close in time and space. That is why annihilation efficiency depends on the cascade size and is higher in the case of heavy ions generating a higher amount of large adjacent cascades. In our opinion, a term could be used to characterize the cascade vicinity is the ion mean free path length between two collisions – the reciprocal mean number of knock-on atoms per unit length,  $1/N_{pka}$ . The mean free path for 710 MeV Bi ions in the silicon substrate of the MOS target equals to 160 Å, as can be deduced from table 3. For example, in the case of 1 MeV Ge ions used in [12] this value is of about 20 Å only. One should note also that authors [12] compared the VO production efficiency in the damage peak region, where the mean free path length was minimal for a given ion-target combination. Therefore, we can suggest that a relatively large distance between collision cascades reduces the annihilation of point defects under hundred MeV ion irradiation and equalizes their number occurring at the same predicted damage dose for light and heavy ions. Further experiments are in progress to check the applicability of this assumption.

## Conclusions

High energy heavy ion irradiation at 300 K enhances the induction of positive charge density in the oxide layer of MOS capacitor structures. A complicated behaviour of the accumulation of radiation defects generating positive charges in the oxide on ionizing density has been observed. The number of electrically active defects being traps for charge carriers strongly decreases under dense electronic excitations. The Q-DLTS spectra analysis showed the relatively equal concentration of vacancy-oxygen centers normalized per displacement cross-section in the silicon substrate of MOS structures irradiated in a wide range of electronic and nuclear stopping power. The similar efficiency of point defect creation monitored by using VO centers density for

hundred MeV Ar and Bi ions is associated with a relatively large mean distance of the collision cascade in comparison with unit MeV heavy ions.

### **Acknowledgements**

Helpful discussions with Professor I. Thurzo and Dr. I. Antonova are gratefully acknowledged. The authors thank Dr. L. Harmatha for offering the samples, V. V. Golikov and E. N. Kulagin for performing neutron irradiation and V. A. Kuzmin for help in calculations of heavy ion damage parameters. This work was partially supported by the Slovak Grant Agency, Project #1/7620/20.

### **References**

1. M. C. Bush, A. Slaoui, E. Dooryhee, and M. Toulemonde, *Rad. Eff. and Def. In Solids* 126, 229-232 (1993).
2. L. Douillard, E. Dooryhee, J-P. Duraud, F. Jollet, and R. A.B. Devine, *Rad. Eff. and Def. In Solids* 126, 237-241 (1993).
3. A. Meftah, F. Brisard, J. M. Constantini, E. Dooryhee, M. Hagi-Ali, M. Hervieu, J. P. Stoquert, F. Studer, and M. Toulemonde, *Phys. Rev.B* 49, 12457-12463 (1994).
4. P. Mary, P. Bogdanski, M. Toulemonde, R. Spohr, and J. Vetter, *Nucl. Instr. Meth. B* 62, 391-393 (1992).
5. A. Dunlop, G. Jaskierowicz, and S. Della-Negra, *Nucl. Instr. Meth. B* 146, 302-308 (1998).
6. B. Canut, N. Bonardi, S. M.M. Ramos, and S. Della-Negra, *Nucl. Instr Meth. B* 146, 296-301 (1998).
7. M. Žiška, L. Harmatha, A. Y. Didyk, V. A. Skuratov, O. Csabay, and J. Staňo, Effect of Hundred MeV Ion Irradiation on MOS Structure in view of Charge DLTS Measurement. Proceedings of the 5th International Workshop, June 23-25, 1999, Kočovce, Slovak Republic
8. J. W. Farmer, C. D. Lamp, and J. M. Messe, *Appl. Phys. Lett.* 44, 1063 (1982).
9. T. J. Mego, *Rev. Sci. Instrum.* 57, 2798 (1986)
10. V. A. Skuratov, A. Illes, Z. Illes, K. Bodnar, A. Yu. Didyk, A. V. Arkhipov, and K. Havancsak, *JINR Communications* E13-99-161, Dubna, p.8 (1999).

11. A. P. Cheplakov, V. V. Golikov, A. Golubyh, G. Ya. Kaskanov, E. N. Kulagin, V. V. Kukhtin, V. I. Lushikov, E. P. Shabalin, E. Leon-Florian, and C. Leroy, Nucl. Instr. Meth. A 411, 330-336 (1998).
12. B. G. Svensson, C. Jagadish, A. Hallén, and J. Lalita, Phys. Rev. B 55, No. 16, 10498 (1997).
13. I. Thurzo and V. Nádaždy, Phys. Status Solidi A 132, 133 (1992).
14. В.И. Авраменко, Ю.В.Конобеев, А.М.Строкова. Нейтронные сечения для расчета повреждающей дозы в реакторных материалах. Атомная Энергия, т.36, вып. 3, с. 139-141
15. L. R. Greenwood, J. Nucl. Mater. 108-109, 21-27 (1982).

Received by Publishing Department  
on March 6, 2001.

Стано Й., Скуратов В.А., Жижка М.

E7-2001-37

Исследование радиационно-индуцированных изменений в МОП-структурах, облученных ионами с энергией  $3 + 7$  МэВ/а.е.м. и быстрыми нейтронами с помощью зарядовой нестационарной спектроскопии глубоких уровней

Методами зарядовой нестационарной спектроскопии глубоких уровней и C-V-измерений исследованы радиационно-индуцированные изменения в МОП-структурах, облученных ионами Bi (710 МэВ), Kr (245 МэВ), Ar (280, 155 МэВ) и быстрыми нейтронами ( $E > 0,1$  МэВ). Установлено, что воздействие высокоэнергетических тяжелых ионов и нейтронов приводит к образованию положительно заряженных состояний в оксидном слое образцов. Плотность этих состояний значительно уменьшается с увеличением уровня электронных возбуждений. Концентрация центров вакансия-кислород в кремниевой подложке, нормированная на полное число дефектов, образованных в упругих соударениях, не зависит от типа частиц.

Работа выполнена в Лаборатории ядерных реакций им. Г.Н.Флерова ОИЯИ.

Сообщение Объединенного института ядерных исследований. Дубна, 2001

Staňo J., Skuratov V.A., Žiška M.

E7-2001-37

Charge Deep Level Transient Spectroscopy Study of  $3 + 7$  MeV/amu Ion and Fast Neutron Irradiation-Induced Changes in Mos Structures

Radiation-induced changes in MOS capacitor structures irradiated with Bi (710 MeV), Kr (245 MeV), Ar (280, 155 MeV) ions and fast neutrons ( $E > 0.1$  MeV) have been studied in view of Q-DLTS and C-V techniques. As was found, high energy ion and neutron irradiation enhance the induction of positive charge density in the oxide layer of MOS samples. The number of electrically active defects in this layer strongly decreases under dense electronic excitations. No dependence of vacancy-oxygen center concentration in silicon substrate normalized per number of displaced atoms by nuclear elastic collisions on projectile type have been observed.

The investigation has been performed at the Flerov Laboratory of Nuclear Reactions, JINR.

Communication of the Joint Institute for Nuclear Research. Dubna, 2001

Макет Т.Е.Попеко

Подписано в печать 04.04.2001  
Формат 60 × 90/16. Офсетная печать. Уч.-изд. листов 1,43  
Тираж 300. Заказ 52576. Цена 1 р. 70 к.

Издательский отдел Объединенного института ядерных исследований  
Дубна Московской области